DRAFT VERSION JANUARY 11, 2019
Typeset using LaTeX **twocolumn** style in AASTeX62

Homogeneous Light Curves for Stars in Clusters from TESS

L. G. BOUMA,[1] W. BHATTI,[1] J. D. HARTMAN,[1] G. Á. BAKOS,[1] AND J. N. WINN[1]

[1] *Department of Astrophysical Sciences, Princeton University, 4 Ivy Lane, Princeton, NJ 08540, USA*

(Received January 11, 2019; Revised —; Accepted —)

Submitted to AAS journals.

ABSTRACT

Lorem ipsum.

Keywords: methods: data analysis — techniques: photometric — (Galaxy:) open clusters and associations: general — planets and satellites: detection

1. INTRODUCTION

Lorem ipsum.

In what follows, § 2 presents BLAH, and § 3 describes BLAH BLAH. § 4 discusses, and § 5 concludes.

2. METHOD

2.1. *Overview*

We reduced the TESS images to lightcurves by performing a sequence of steps using stand-alone programs. A conceptual overview of our "pipeline" is given in Figure 2. Similar pipelines have been presented by Pál (2009), Soares-Furtado et al. (2017) and Oelkers & Stassun (2018).

We begin with the calibrated full frame images produced by SPOC (§ 2.2). We then perform a collection of preparatory steps, including source extraction of bright stars, astrometry using the resulting positions, and coarse simple aperture photometry (§ 2.3). Using the shape values from the initial astrometry, we select an astrometric reference frame and transform all of the calibrated images to it. We construct a photometric reference by stacking a collection of frames, and then convolve all the transformed frames to match the photometric reference, and subtract (§ 2.4). We perform aperture photometry on the subtracted images using positions projected onto the frame from Gaia DR2. We detrend the resulting lightcurves (§ 2.5) in two subsequent steps. First, we apply External Parameter Decorrelation (EPD, Bakos et al. 2010), and then we apply a Trend Filtering Algorithm (TFA, KovÃącs et al. 2005). Finally, we assess the resulting lightcurves using a variety of statistics for their white noise and red noise properties (§ 3).

2.2. *Observations*

Corresponding author: L. G. Bouma
luke@astro.princeton.edu

The TESS spacecraft began science operations on July 25, 2018. To keep its cameras pointed opposite the Sun, the spacecraft advances by ≈28 degrees in ecliptic longitude every lunar month. Data acquired throughout each "sector" is downlinked at spacecraft perigee through the Deep Space Network. Verbose descriptions of the spacecraft's design and operations are given by Ricker et al. (2015) and the instrument handbook (Vanderspek et al. 2018).

For us, the main data product of interest is the calibrated full frame image (FFI). Each TESS camera reads out every 2 seconds. To produce a manageable telemetric load, the resulting pixel values are summed by the onboard computer into 30 minute averages. (An on-board cosmic ray mitigation algorithm is applied.) Once transmitted to the ground, the raw images are calibrated by the Science Processing Operations Center. The calibration process includes an overscan, bias, and dark current correction, and also dividing out a flat field. The details are given by Clarke et al. (2017), and the resulting science data products are described by Tenenbaum & Jenkins (2018).

We begin our analysis using the calibrated images, their uncertainty maps, and their associated headers. The spacecraft has four cameras, and each camera has four CCDs. In the following analysis, all image-level operations are thus performed on the images for each CCD, so that at any instant of time there are 16 independent images undergoing analysis.

2.3. *Preparatory Steps*

Before we can perform any kind of photometry, a few janitorial tasks are required.

The first is to trim and mask the images. We convert the calibrated image from MAST into a `fitsh`-compatible image by retrieving the image data (omitting the uncertainty map, for now). We then trim the image to remove virtual rows and columns (using the `SCIROWS`, `SCIROWE`, `SCCSA`, `SCCED`, header values). We then mask out saturated stars using the 'fiign' program with a fixed saturation level of

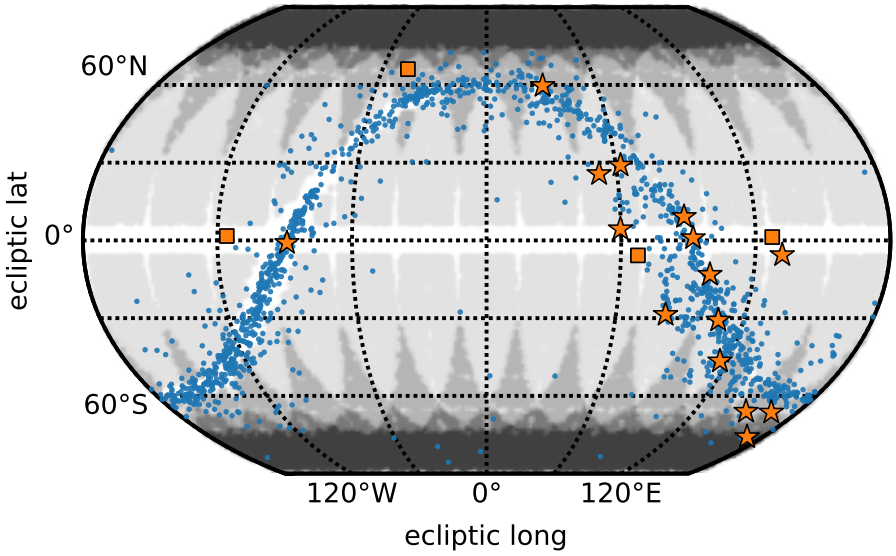

Figure 1. There are many clusters; TESS looks at them. Placeholder skymap.

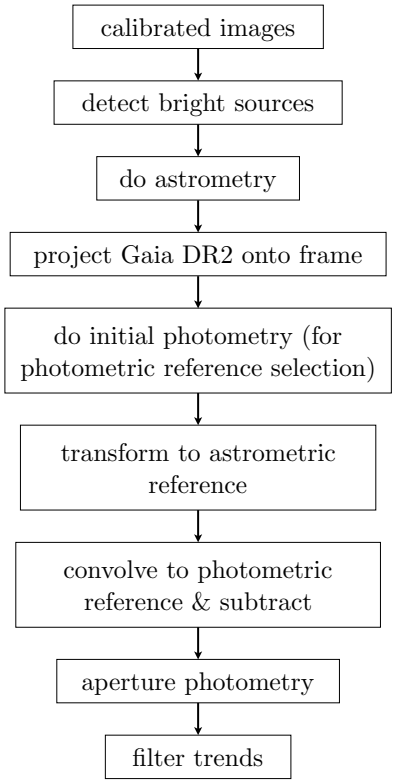

Figure 2. Pipeline. This is what we do.

2^{16} ADU. As described by Pál (2009), the mask is metadata to the image, and is not actually applied to the pixel values. During masking, we also use the algorithm described by Pál (2009) to extend masks beyond purely satured pixels to "bloomed" pixels – pixels horizontally and vertically adjacent to the saturated pixels. Finally, for frames with the `DQUALITY` bit-flag set to 32 — corresponding to the "momentum dumps" described by Vanderspek et al. (2018) — we mask out the entire frame. This removes on average a few frames per sector. Through visual inspection, we see that the stars on these frames are extremely smeared, and are unlikely to produce useful science data.

Next, we perform some initial analysis steps to produce metadata needed during image subtraction. To obtain an astrometric solution (independent from the WCS data packaged with the frames), we use `fistar` to perform source extraction on bright stars in each image. We pass the resulting source lists through `astrometry.net` (Lang et al. 2010), which returns an astrometric solution for each frame packaged in the WCS format (Pence et al. 2010, Sec. 8). During the initial source extraction, we also fit elongated gaussians to the bright stars, yielding the shape parameters (S,D,K), where the flux as a function of position is assumed to take the form

$$f_{\rm elong}(\vec{x}) = B + A\exp\{-0.5\times(S(\Delta x^2+\Delta y^2)+ \quad (1)$$

$$D(\Delta x^2-\Delta y^2)+K(2\Delta x\Delta y))\}, \quad (2)$$

for $\Delta x = x - x_0$, and $\Delta y = y - y_0$. S is typically called the "sharpness". For a nearly circular shape profile, FWHM $\approx 2.35\sqrt{S}$ (*e.g.*, Pál 2009). These shape parameters are later used when selecting an astrometric reference (§ 2.4)

With the resulting WCS information, we then project a source catalog from Gaia-DR2 onto the frame, down to a preselected magnitude cutoff (Gaia Collaboration et al. 2018). We use these expected positions to center the apertures in our photometry, rather than attempting to detect the positions. Such "forced-aperture photometry" is preferable to performing source extraction because of the large TESS pixels, and the accurate Gaia positions. The Gaia-DR2 epoch is J2015.5, so even the fastest-moving stars with proper motions of $\sim$1 arcsecond yr^{-1} are still well within one pixel of

their predicted positions in the TESS images. The projection and catalog-indexing is performed using `gaia2read`[1] (CITE Jason Kim junior thesis).

Finally, we perform aperture photometry on the bright stars from the source list, by summing the counts inside appropriately-weighted circular apertures centered on the projected positions from Gaia DR2. The pixel weights $w_{x,y}$ are equal to the fraction of the pixel that falls within the aperture. They are thus unity for pixels entirely within the aperture, and fractional along the aperture boundary (e.g., Pál 2009 Fig 17). The background levels are measured in annuli around each aperture center. The raw flux of the object after background removal is then (Pál 2009 Eq 65)

$$f = \sum_{x,y} w_{x,y}(I_{x,y} - B) = f_{\rm total} - B r_0^2. \quad (3)$$

The resulting measurements, for instance of the background level of each aperture, and the number of "good" objects that are detected, are later used as input for selecting photometric reference frames.

2.4. *Image Subtraction*

We then select two "reference frames" for image subtraction. The first is the astrometric reference; the second is the photometric reference. To choose the astrometric reference, we use the following heuristics:

1. The frame must have large and round stars (largest "S", smallest "D" and "K" values).
2. The frame must minimal background noise, as measured in annuli around the bright stars selected in § 2.3.
3. The frame must have, relative to the other frames being considered, a large number of detected sources.

We sort the frames using the above metrics, and then select the astrometric reference from successive intersections of each sorted list. Using the algorithm presented by Pál & Bakos (2006), we then calculate a spatial transformation that maps the X and Y coordinates from each calibrated frame onto the the astrometric reference.

"Registering" the images onto a common astrometric reference frame requires some care. In particular, the transformation must preserve the fluxes of the sources. Since the transformation is affine (a combination of *e.g.*, translation, rotation, dilation, and shear) standard bilinear or bicubic interpolation would not achieve flux conservations. We therefore use the flux-conserving interpolation scheme described by Pál (2009) which is based on analytic integration of the surfaces determined by the pixel values. The largest component of the transformation is a translation, of order 2 arcseconds, or about 0.1 TESS pixels.

The second reference frame needed for image subtraction is the photometric reference. This is a high-SNR median average of frames that is used both to calculate the convolution kernel during image subtraction, and to measure the reference flux of each star. To select viable frames for inclusion in the photometric reference, we use the results of our initial photometry step (§ 2.3), and sort frames for each sector by:

1. Lowest median scatter in photometry
2. Lowest median error in photometry
3. Lowest median background measurement
4. Lowest median absolute deviation in background measurements
5. Largest number of stars detected by `fiphot` with good flags.

We convolve the 50 best candidate photometric references to the best photometric reference, and then perform a median combination of the frames to make the photometric reference.

Some details of, and motivation for, the convolution process are warranted. The general idea of the image subtraction problem is to...

This has some benefits for crowded regions. Most notably, in enables a measurement of the background flux level.

Our approach follows from the algorithm presented by Alard & Lupton (1998), and explained in detail by Miller et al. (2008). The process is:

1. Select a set of isolated stars ("stamps").
2. Choose basis vectors K_n for the kernel, $K = \sum_{n=1}^{N} a_n K_n$. Our goal is to determine the best-fitting coefficients a_n.
3. Using these stamps and the least-squares method, ...

Finally, we convolve and subtract all the frames that have been translated from the photometric reference (`grcombine`). We use the same kernel formalism as described by Soares-Furtado et al. (2017). To compute the convolution kernel, we minimize the difference between each image and the photometric reference (or something like this), using the Alard & Lupton 1998 method (CITE, also CITE Miller's reference). The software implementation is that by Pál (2009), in the `ficonv` program. The implemented math is as follows.

$$XXX = XXX. \quad (4)$$

We explored a variety of kernel options, including X, Y, and Z. We wound up including an "identity" term (MEANING?), a "background term" (MEANING?) and a delta function term (MEANING? Give math for all of these). There are also spatially-varying terms of order XX. (MEANING?)

We perform forced-aperture photometry on the subtracted frames, using the locations from the Gaia projection, to measure the resulting difference fluxes. We use circular apertures, with the appropriate weigths along the boundaries (`fiphot`; Pál (2009) Section FIXME).

Note that to measure the fluxes on the differenced images, a slightly different procedure from Eq. 3 is relevant. (Pal

[1] github.com/samuelyeewl/gaia2read

2009 Section 2.9). Specifically, the subtracted image S is given by $I - B - R * K$, for I the original image, B the background, R the reference image, and K the convolution kernel. The flux in the original image is given by

$$f = \sum_{x,y} w_{x,y} I_{x,y} \tag{5}$$

$$= \frac{1}{||K||_1^2} \sum_{x,y} S_{x,y}(w * K)_{x,y} + \sum_{x,y} R_{x,y} w_{x,y}, \tag{6}$$

Finally, to convert from a list of sources on each frame to a list of flux values at any given time, we use the `grcollect` transposition tool.

2.5. *Lightcurve Detrending*

The preceding tedium produces lightcurves that include both instrumental systematics as well as astrophysical variability. To remove the systematics, we perform two subsequent detrending steps: we decorrelate against "external parameters" (EPD, CITE) that we know affect the stellar flux measurements, and then we filter remaining systematic trends from unknown parameters (TFA, CITE). While these processes have been described at length by CITE, CITE, and CITE, we briefly summarize them here for self-consistency.

In "external parameter decorrelation", we fit the flux for each star as a function of $(x, y, \{x\}, \{y\}, |F|, T)$ (positions, fractional positions, amplitude of flux, spacecraft temperature, etc). Specifically, we fit a model

$$m = a_s S + a_s 2S^2 + a_d D + a_d 2D^2 + a_k K + a_k 2K^2 + const + a_s dS * D + a_s kS * K + a_d kD * K + a_x \sin(2\pi x) + b_x \cos(2\pi x) + a_y \sin(2\pi y) + b_y \cos(2\pi y) + a_2 x \sin(\tag{7}$$

to the magnitudes m through linear least squares.

$$XXX = XXX, \tag{8}$$

and we do something like least squares to get the best-fitting coefficients.

In "trend filtering", we correlate the flux timeseries of each star against other stars in the frame (Kovacs et al, CITE). This requires selecting "template stars", which are a subsample of star that are supposed to represent all the types of systematics across the dataset. We select 500 template stars randomly from the stars on-chip with G_{R_p} magnitudes between 8.5 and 13 (TODO: rather bright?). We additionally require these stars to not have excessive variability, by fitting a parabola in the RMS-magnitude plane, and discarding stars more than 4σ away from the prediction of this fit.

Once the template stars are selected, we use the secret TFA implementation from the `HATpipe` source code, that you and nobody else is allowed to see.

To select template stars, we impose a

The details of this selection procedure are

3. RESULTS

RMS vs mag plots.

SNR of retrieved HJs.

Some stellar variability plots (perhaps of known stellar variables).

Some focus on actual cluster fields.

4. DISCUSSION

Lorem ipsum.

5. CONCLUSION

L.G.B. gladly acknowledges helpful discussions with ..., and is grateful to the people who have turned TESS from an idea into reality. J.N.W. thanks ... This paper includes data collected by the TESS mission, which are publicly available from the Mikulski Archive for Space Telescopes (MAST). Funding for the TESS mission is provided by NASA's Science Mission directorate. This research has made use of the NASA Exoplanet Archive, which is operated by the California Institute of Technology, under contract with the National Aeronautics and Space Administration under the Exoplanet Exploration Program. This work made use of NASA's Astrophysics Data System Bibliographic Services. This research has made use of the VizieR catalogue access tool, CDS, Strasbourg, France. The original description of the VizieR service was published in A&AS 143, 23. This work has made use of data from the European Space Agency (ESA) mission *Gaia* (https://www.cosmos.esa.int/gaia), processed by the *Gaia* Data Processing and Analysis Consortium (DPAC, https://www.cosmos.esa.int/web/gaia/dpac/consortium). Funding for the DPAC has been provided by national institutions, in particular the institutions participating in the *Gaia* Multilateral Agreement.

Facility: TESS (Ricker et al. 2015), Gaia (Gaia Collaboration et al. 2016, 2018)

Software: `astrobase` (Bhatti et al. 2018), `astropy` (Collaboration et al. 2018), `astroquery` (Ginsburg et al. 2018), `BATMAN` (Kreidberg 2015), `corner` (Foreman-Mackey 2016), `emcee` (Foreman-Mackey et al. 2013), `fitsh` (Pál 2012), `IPython` (Pérez & Granger 2007), `matplotlib` (Hunter 2007), `numpy` (Walt et al. 2011), `pandas` (McKinney 2010), `scipy` (Jones et al. 2001).

REFERENCES

Alard, C., & Lupton, R. H. 1998, ApJ, 503, 325

Bakos, G. A., Torres, G., Pál, A., et al. 2010, The Astrophysical Journal, 710, 1724

Bhatti, W., Bouma, L. G., & Wallace, J. 2018, `astrobase`

Clarke, B. D., Caldwell, D. A., Quintana, E. V., et al. 2017, Kepler Science Document, 5

Collaboration, T. A., Price-Whelan, A. M., Sipöcz, B. M., et al. 2018, arXiv:1801.02634 [astro-ph], arXiv: 1801.02634

Foreman-Mackey, D. 2016, The Journal of Open Source Software, 24

Foreman-Mackey, D., Hogg, D. W., Lang, D., & Goodman, J. 2013, Publications of the Astronomical Society of the Pacific, 125, 306

Gaia Collaboration, Prusti, T., de Bruijne, J. H. J., et al. 2016, Astronomy and Astrophysics, 595, A1

Gaia Collaboration, Brown, A. G. A., Vallenari, A., et al. 2018, Astronomy and Astrophysics, 616, A1

Ginsburg, A., Sipocz, B., Madhura Parikh, et al. 2018, Astropy/Astroquery: V0.3.7 Release

Hunter, J. D. 2007, Computing in Science & Engineering, 9, 90

Jones, E., Oliphant, T., Peterson, P., et al. 2001, Open source scientific tools for Python

KovÃącs, G., Bakos, G., & Noyes, R. W. 2005, Monthly Notices of the Royal Astronomical Society, 356, 557

Kreidberg, L. 2015, Publications of the Astronomical Society of the Pacific, 127, 1161

Lang, D., Hogg, D. W., Mierle, K., Blanton, M., & Roweis, S. 2010, The Astronomical Journal, 139, 1782

McKinney, W. 2010, in Proceedings of the 9th Python in Science Conference, ed. S. van der Walt & J. Millman, 51

Miller, J. P., Pennypacker, C. R., & White, G. L. 2008, Publications of the Astronomical Society of the Pacific, 120, 449

Oelkers, R. J., & Stassun, K. G. 2018, The Astronomical Journal, 156, 132

Pál, A. 2009, PhD thesis, arXiv: 0906.3486

—. 2012, MNRAS, 421, 1825

Pál, A., & Bakos, G. A. 2006, Publications of the Astronomical Society of the Pacific, 118, 1474

Pence, W. D., Chiappetti, L., Page, C. G., Shaw, R. A., & Stobie, E. 2010, Astronomy and Astrophysics, 524, A42

Pérez, F., & Granger, B. E. 2007, Computing in Science and Engineering, 9, 21

Ricker, G. R., Winn, J. N., Vanderspek, R., et al. 2015, Journal of Astronomical Telescopes, Instruments, and Systems, 1, 014003

Soares-Furtado, M., Hartman, J. D., Bakos, G. Ã., et al. 2017, Publications of the Astronomical Society of the Pacific, 129, 044501

Tenenbaum, P., & Jenkins, J. 2018, TESS Science Data Products Description Document, EXP-TESS-ARC-ICD-0014 Rev D, https://archive.stsci.edu/missions/tess/doc/EXP-TESS-ARC-ICD-TM-0014.pdf

Vanderspek, R., Doty, J., Fausnaugh, M., et al. 2018, TESS Science Document

Walt, S. v. d., Colbert, S. C., & Varoquaux, G. 2011, Computing in Science & Engineering, 13, 22